Supporting Information For:

Self-assembly of neutral platinum complexes controlled by thermal inputs

Masaya Yoshida,[†] Takehiro Hirao,[†] and Takeharu Haino[*]

Department of Chemistry, Graduate School of Advanced Science and Engineering, Hiroshima University, 1–3–1 Kagamiyama, Higashi-Hiroshima, Hiroshima, 739-8526, JAPAN.

To whom correspondence should be addressed: *E-mail: haino@hiroshima-u.ac.jp

[†]These two authors contributed equally.

Contents

General

All solvents were commercial reagent grade and were used without further purification. UV/vis absorption spectra were recorded on a JASCO V-560 spectrometer. Fluorescence spectra were measured using a JASCO FP-6500 spectrometer. Circular dichroism (CD) spectra were recorded on a JASCO J-1500 spectrometer. Dynamic Light Scattering (DLS) analysis was performed on a Malvern zetasizer nanoZS instrument. Atomic force microscopic (AFM) images were observed using a Keysight Technologies PicoView5100 microscope in air at ambient temperature with a Bruker cantilever model NCHV in the tapping mode. WSxM software[1] was used for the AFM image analysis. Morphological evaluation of the samples was performed using scanning transmission electron microscopy (STEM) using JEOL JEM-2100F and field-emission scanning electron microscopy (SEM) using a Hitachi High-Technologies S-5200. Previously synthesized (*S*)-, (*R*)-**1**[2] and **2**[3] were used for this work.

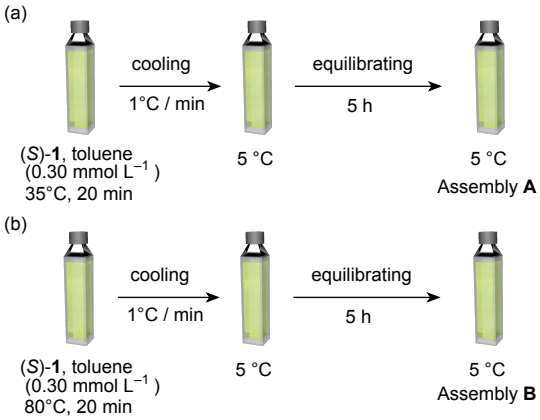

Figure S1. Schematic illustration of the preparation protocol of (a) assembly **A** and (b) assembly **B**.

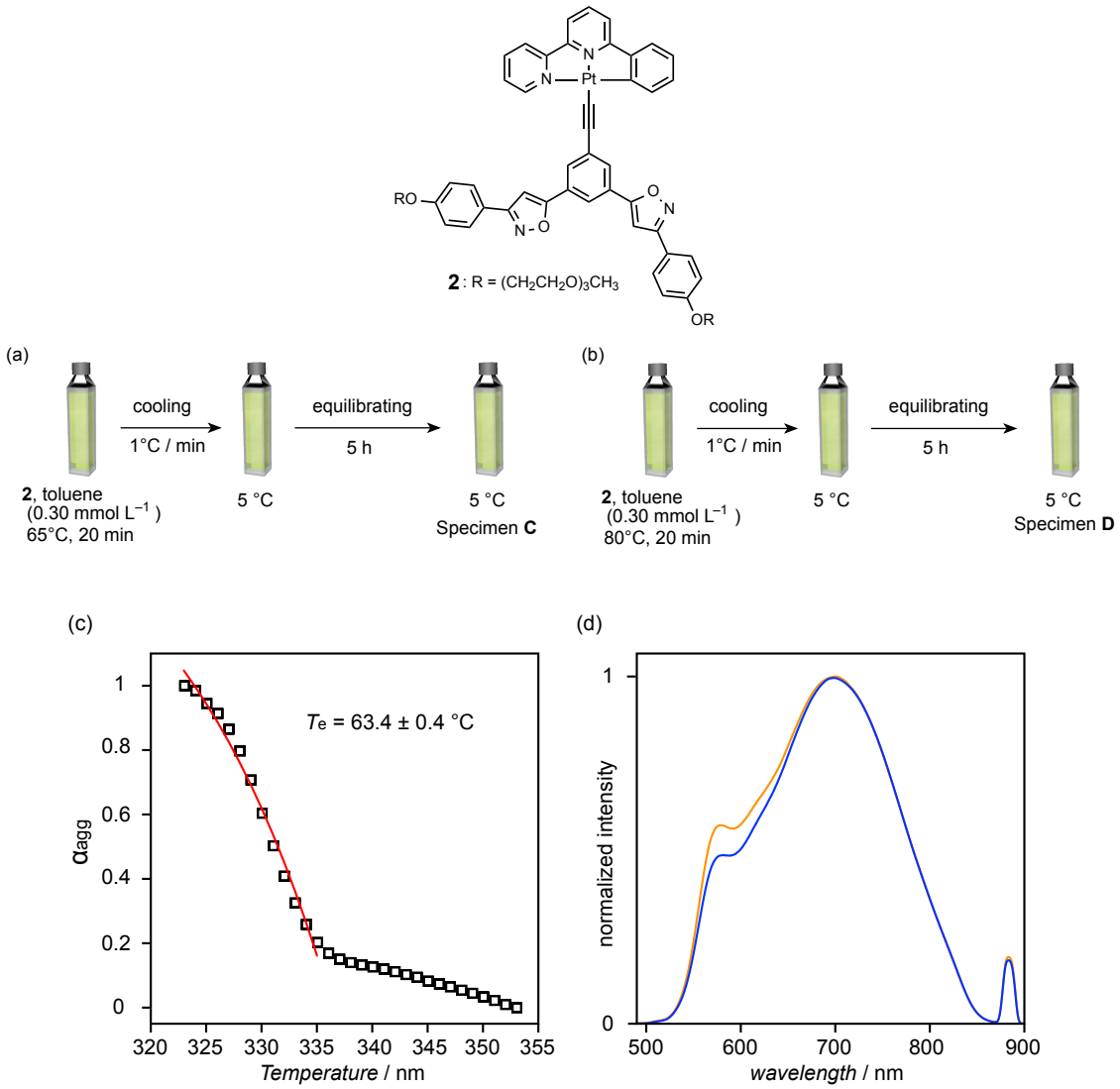

Figure S2. Schematic illustration of the preparation protocol of (a) specimen **C** and (b) specimen **D**. (c) Plot of degree of aggregation (α_{agg}) estimated from absorbance value at 447 nm against temperature and the fitting curve of the elongation stage obtained by van der Schoot's model[4], where α_{agg} was calculated according to the following equation: $\alpha_{agg} = (Abs_{obs} - Abs_{50°C})/(Abs_{80°C} - Abs_{50°C})$. The data points were obtained in the heating run. (d) Normalized emission spectra (λ_{ex} = 444 nm) of (orange) specimen **C** and (blue) specimen **D**.

A control experiment using **2** was carried out. **2** formed assemblies through nucleation-elongation process. The T_e was determined to be 63.4 ± 0.4 °C. Based on the T_e value, two specimens were prepared as shown in panels (a) and (b). The wave form of the emission spectrum of specimen **C** was consistent with that of specimen **D**, suggesting that peripheral chiral moieties were crucial for the emergence of the pathway complexity.

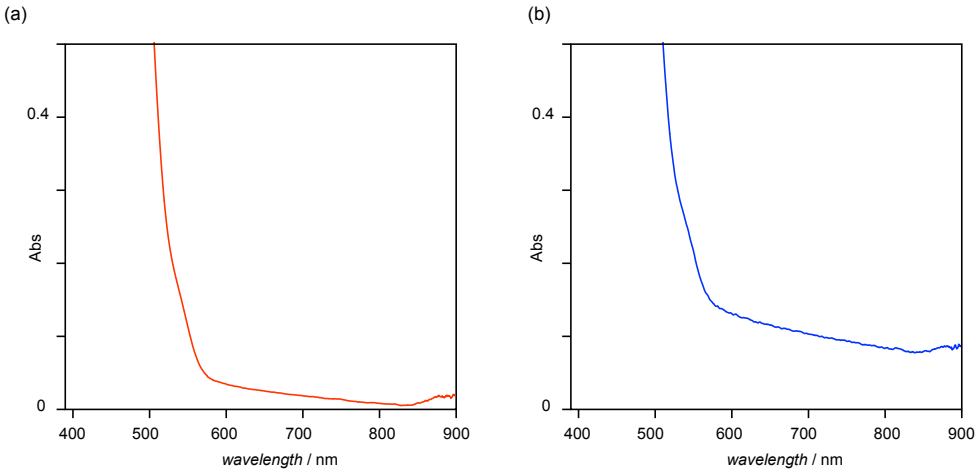

Figure S3. Expanded view of UV/vis spectra of (a) assembly **A** and (b) assembly **B** at 25 °C in toluene.

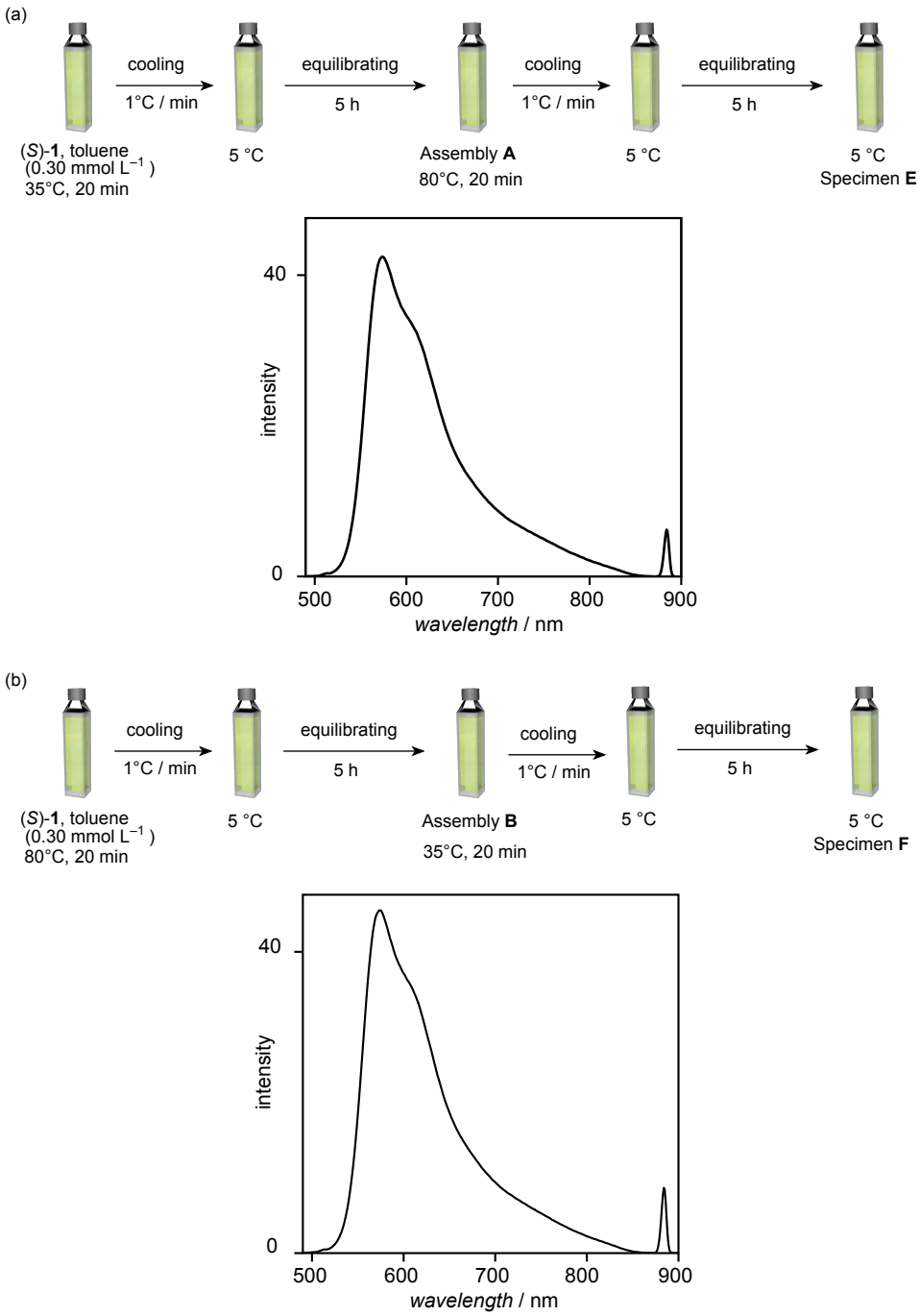

Figure S4. Emission spectra of (a) specimen **E** and (b) specimen **F**, both of which illustrated the spectra consistent with assembly **B**.

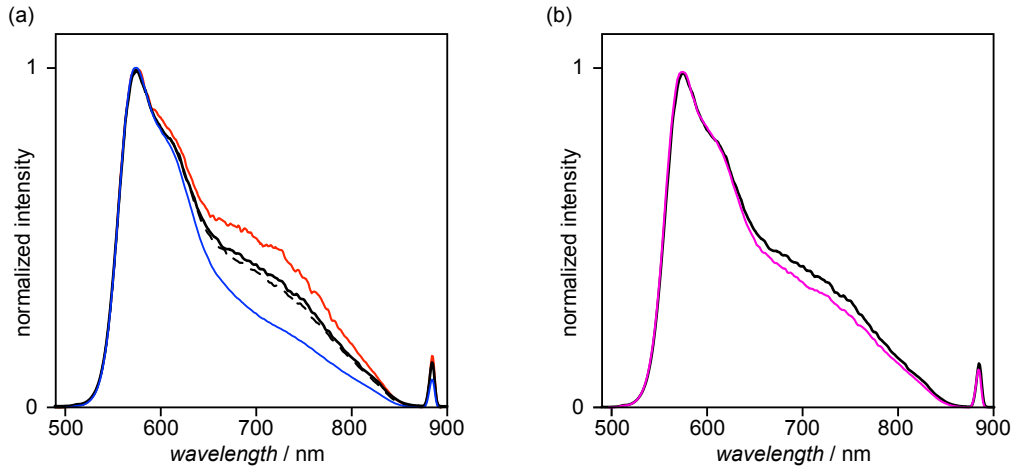

Figure S5. (a) Normalized emission spectra of (red) assembly **A**, (blue) assembly **B**, (black broken line) a 1:1 mixture of assembly **A** and assembly **B** right after prepared, and (black solid line) a 1:1 mixture of assembly **A** and assembly **B** after equilibrating for 350 min. (b) Comparison between (black) the normalized emission spectrum of a 1:1 mixture of assembly **A** and assembly **B** after equilibrating for 350 min and (purple) the normalized spectrum obtained by mathematical summation of emission spectra of assembly **A** and assembly **B**.

An emission spectrum of the mixture right after prepared was illustrated in between the spectra seen in the solutions of assembly **A** and assembly **B**. Minimal changes were observed in the spectrum after equilibrating for 350 min. The resulting spectrum is in good agreement with the simulated spectrum obtained by mathematical summation of emission spectra of assembly **A** and assembly **B**, indicating that both of the assemblies are not interconvertible in toluene at 25 °C at least 350 min.

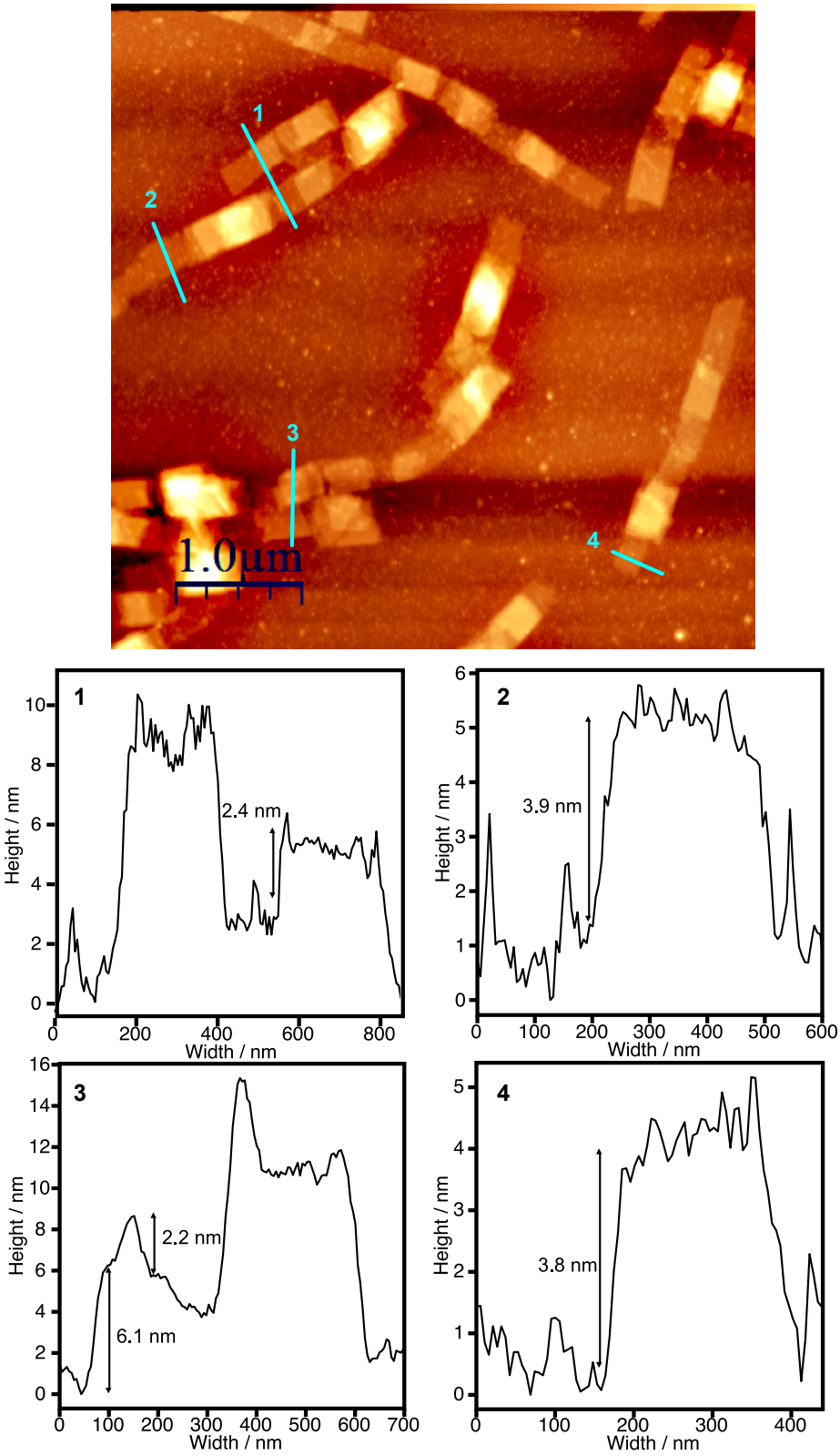

Figure S6. AFM image of assembly **A** on mica and the height profiles of the plate-like structures.

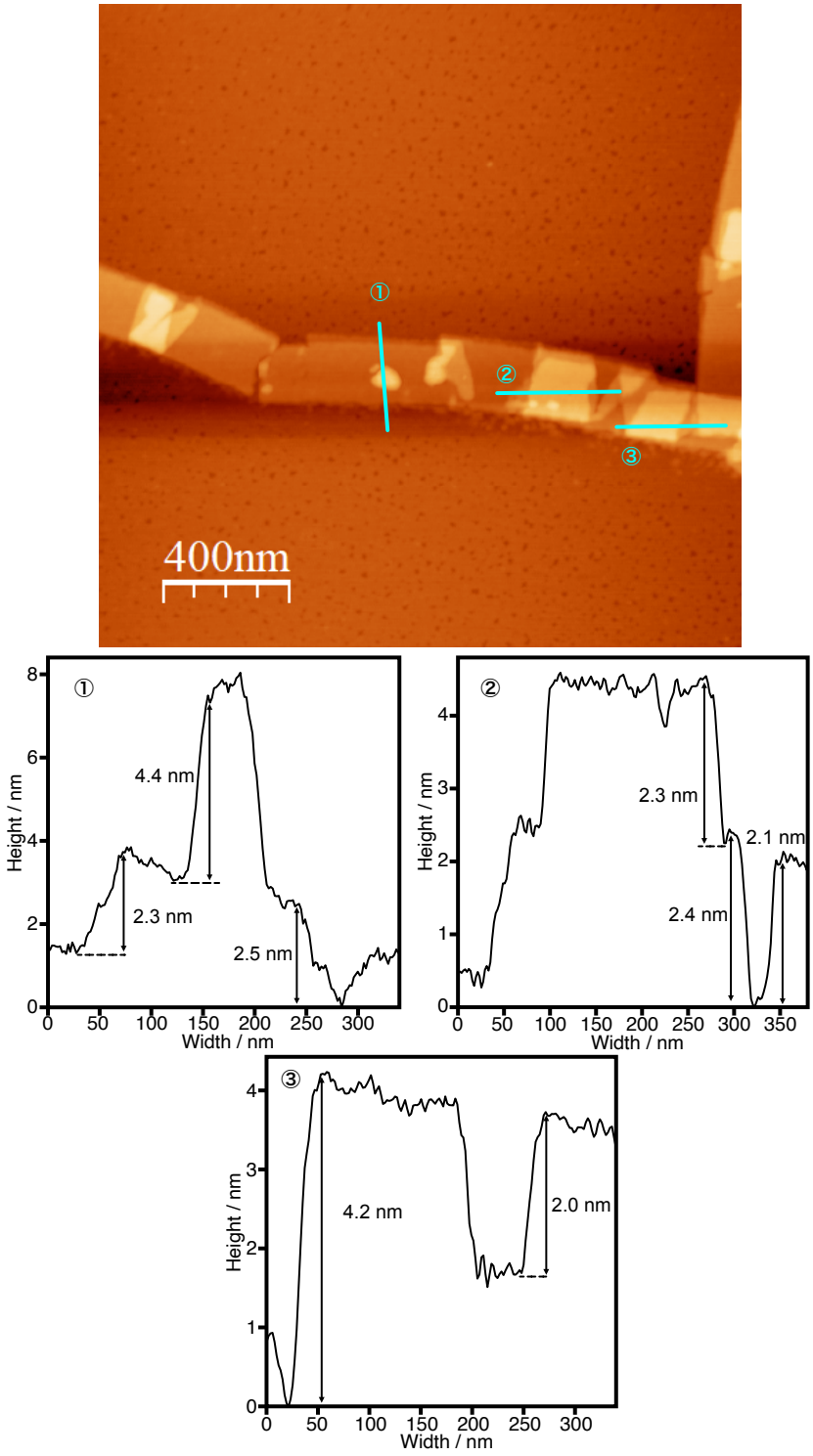

Figure S7. AFM image of assembly **A** on mica and the height profiles of the plate like structures.

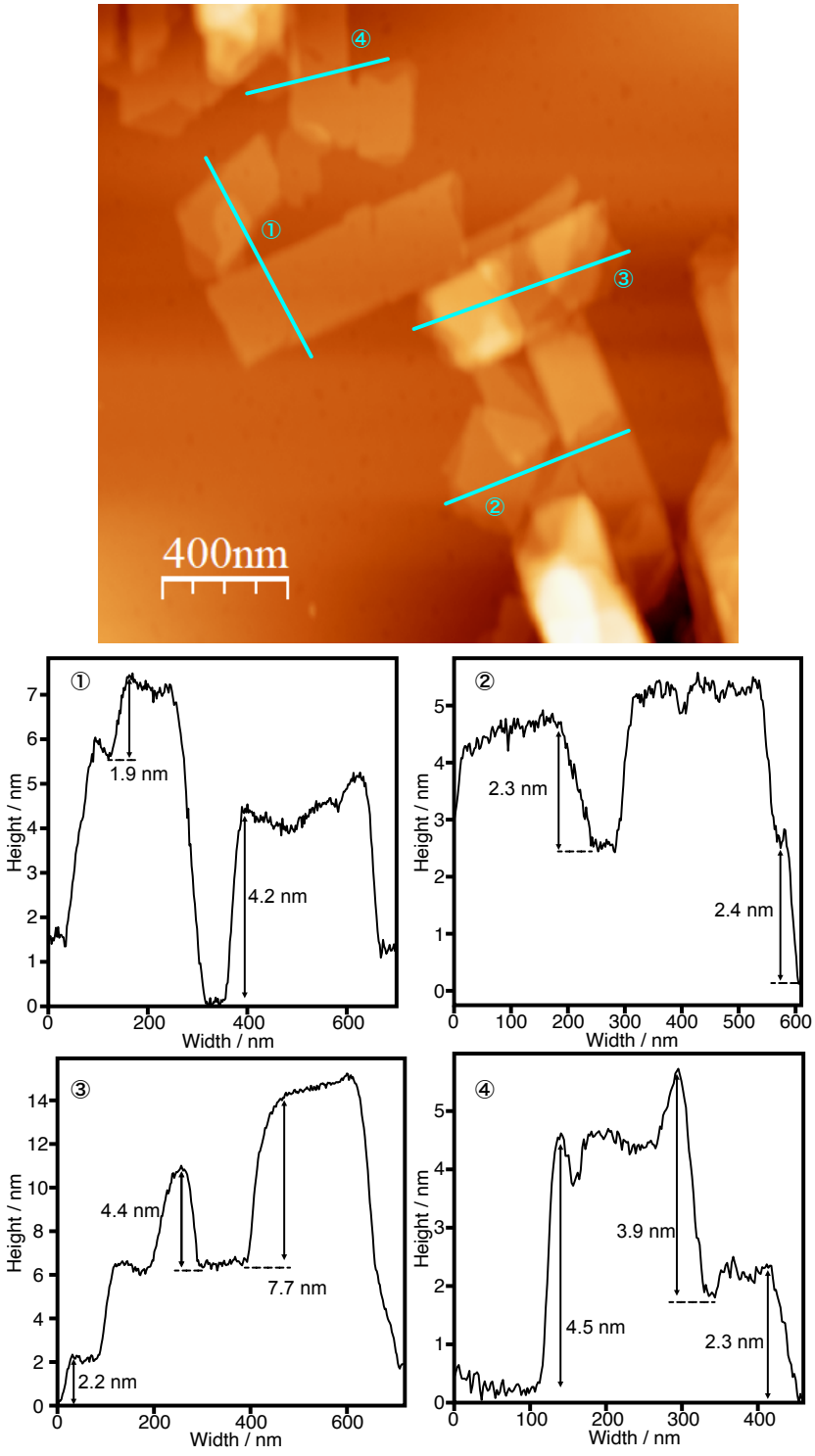

Figure S8. AFM image of assembly **A** on mica and the height profiles of the plate like structures.

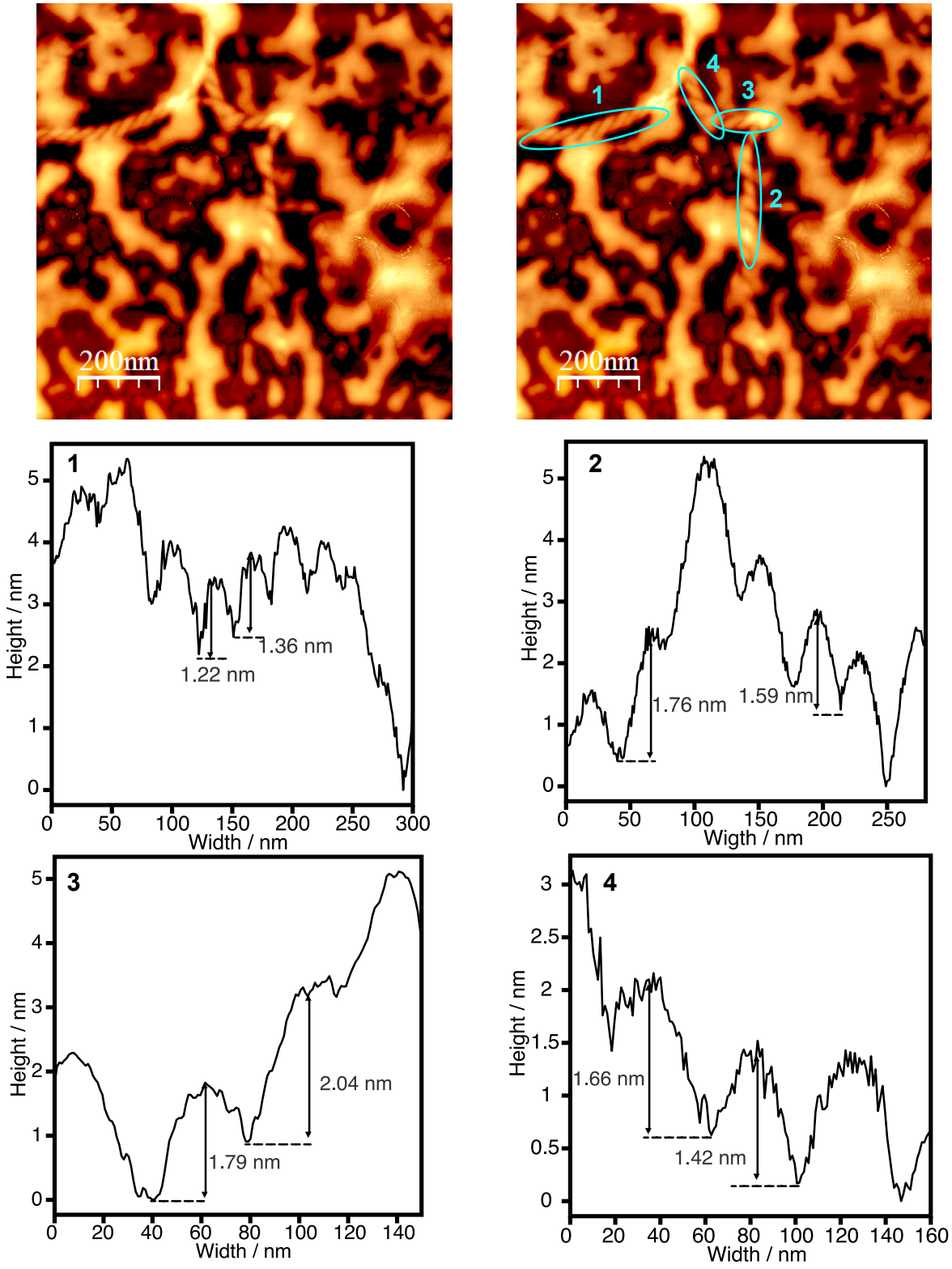

Figure S9. AFM image of assembly **B** on mica and the height profiles of the helices. The blue circles highlight the left-handed helices.

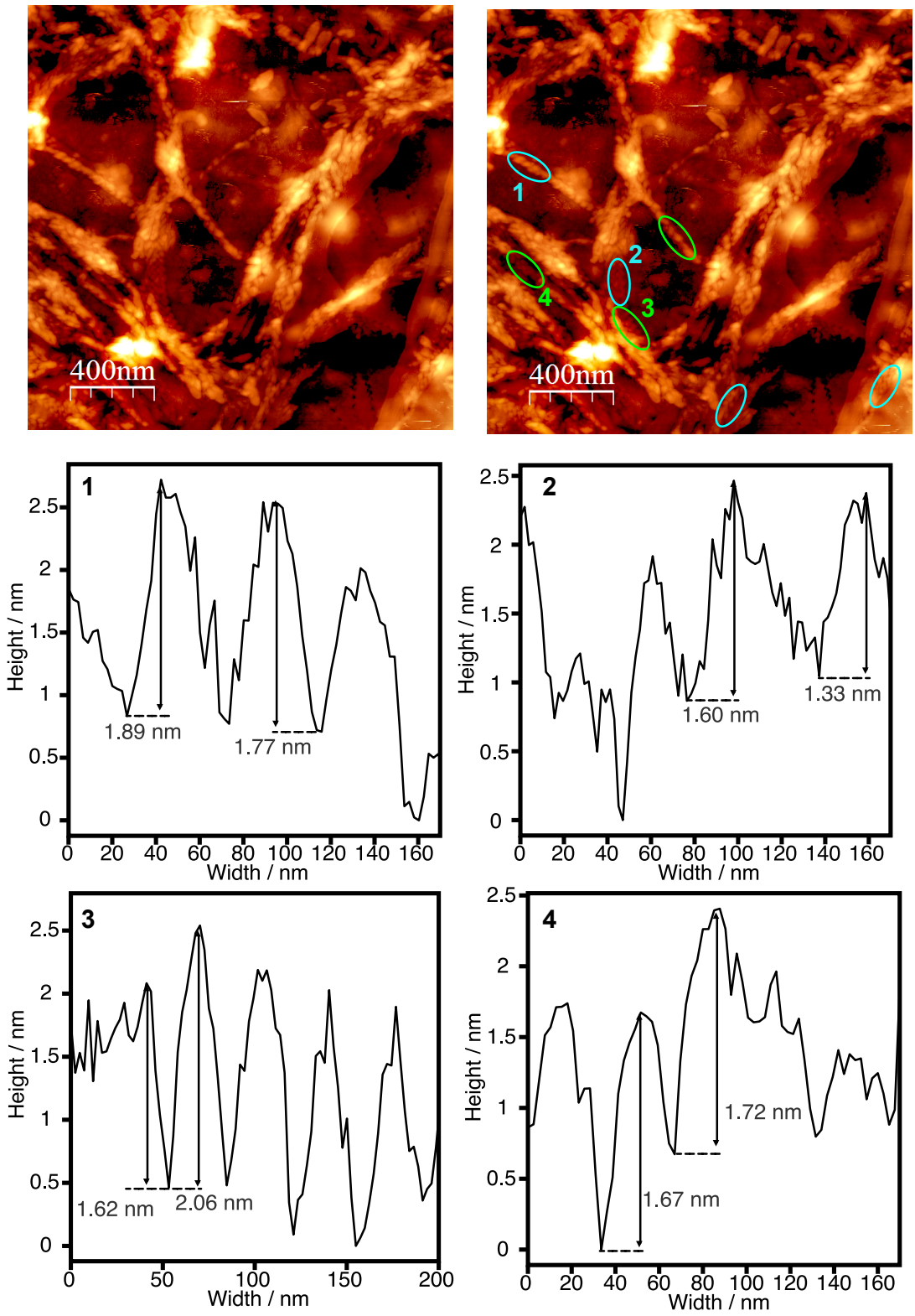

Figure S10. AFM image of assembly **B** on mica and the height profiles of the helices. The blue and green circles highlight the left-handed and right-handed helices, respectively.

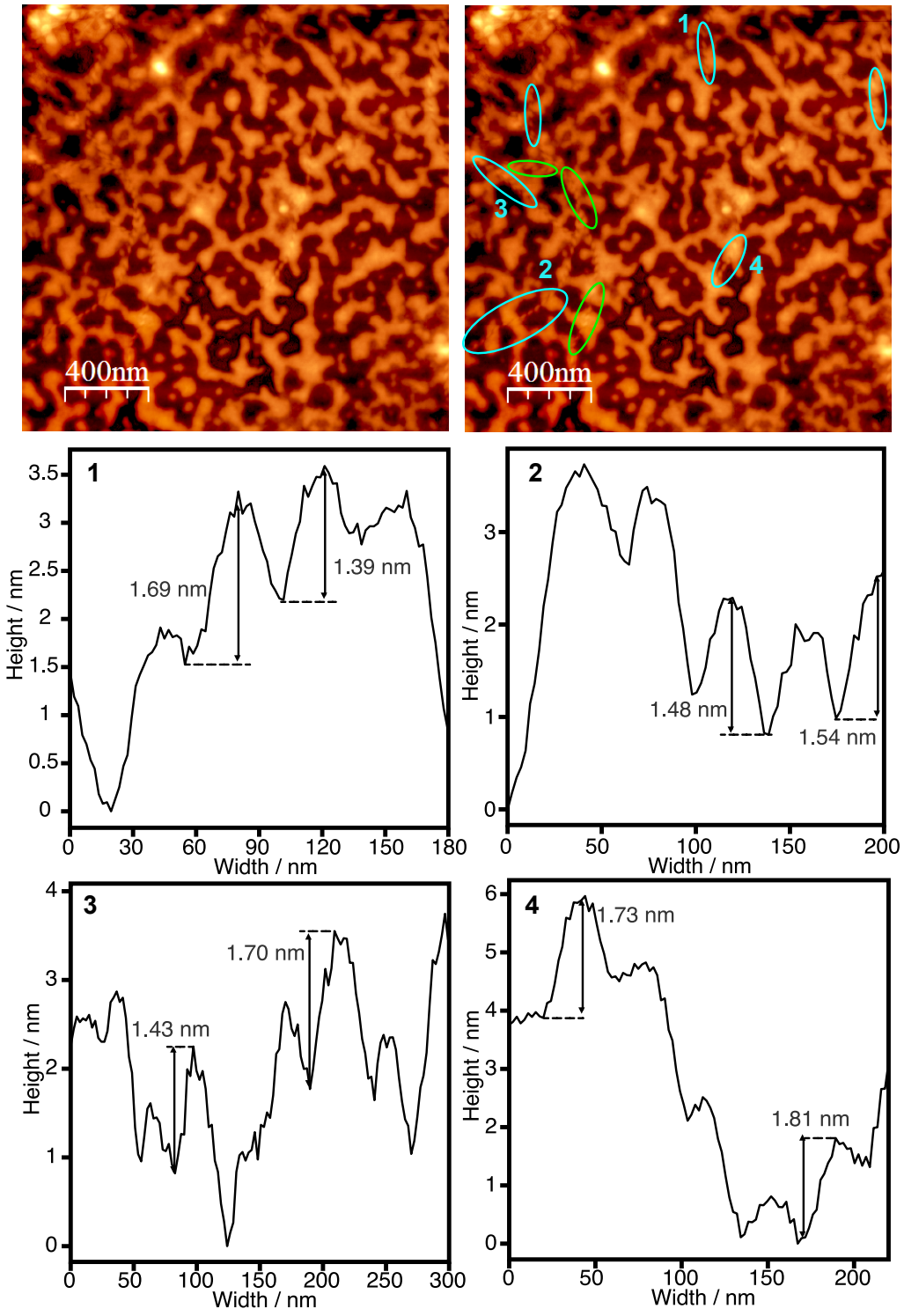

Figure S11. AFM image of assembly **B** on mica and the height profiles of the helices. The blue and green circles highlight the left-handed and right-handed helices, respectively.

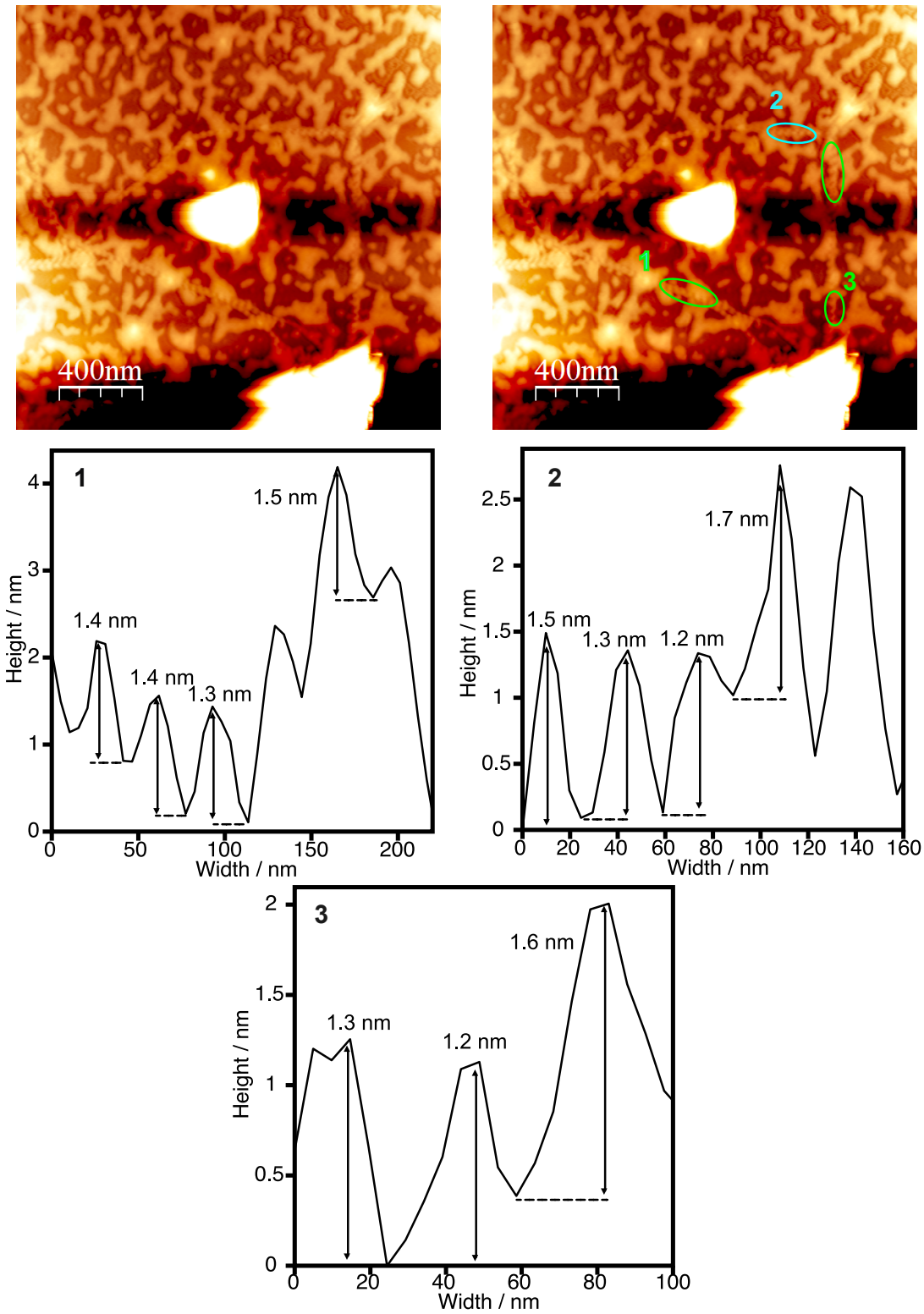

Figure S12. AFM image of assembly **B** on mica and the height profiles of the helices. The blue and green circles highlight the left-handed and right-handed helices, respectively.

Table S1. Randomly picked up height of fibers observed in the AFM images shown in Figure S2–S4.

Height of polymer / nm	Height of polymer / nm	Height of polymer / nm	Height of polymer / nm	Height of polymer / nm
1.20789748	1.42994915	1.48202787	1.4148268	1.33116421
0.98720391	1.17951655	1.19536542	1.09690045	1.61871022
0.9974123	1.29961476	1.542869	1.15374156	2.05985967
1.21521089	1.26521179	2.09020171	1.05029921	2.01223429
1.36299773	1.58811646	1.84479332	1.16783125	1.93804627
1.25215598	1.54578457	1.43002141	1.87556015	1.89568512
1.75810796	1.16481533	1.40843142	2.11781538	1.73879629
1.42938054	1.74490699	1.70062082	1.72669294	1.67376782
1.69775672	1.29741453	1.34224659	1.16641717	1.72202451
2.11533636	1.38579215	1.72832776	1.54373979	**Average** 1.54 ± 0.03
1.5936924	1.17466932	2.71700479	1.54740261	
2.12449777	1.19244744	1.97109373	1.8940564	
1.79085464	1.30704655	1.81265119	1.53335471	
2.04822184	1.16299898	1.47569714	1.88823046	
1.77230719	1.18437849	1.25289611	1.76567558	
1.65706998	1.81704597	1.77426532	1.86791943	
1.41797618	1.68539262	2.09530704	1.91704061	
1.35095018	1.39193664	1.40649614	1.59884576	

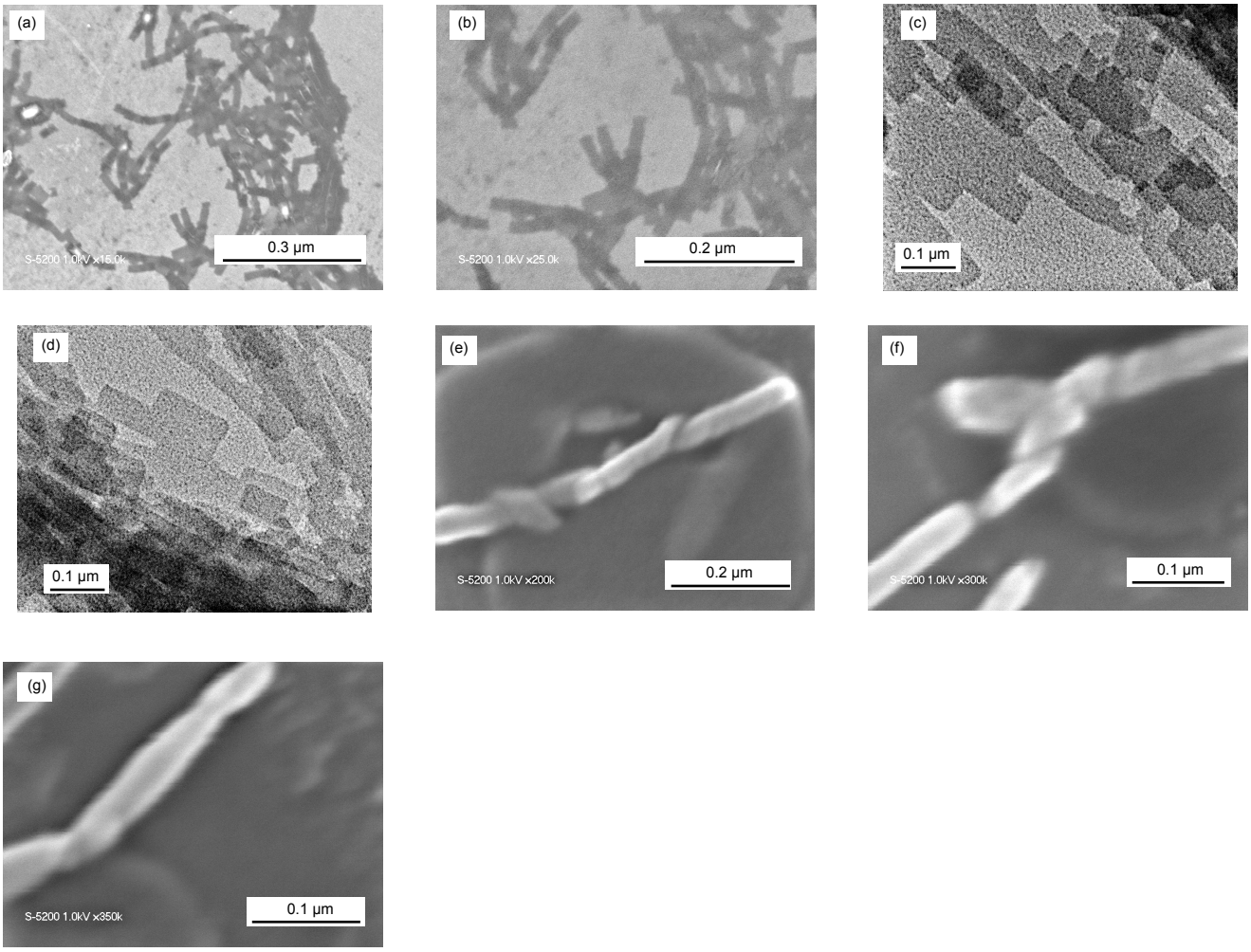

Figure S13. (a, b) Scanning electron microscopic (SEM) and (c, d) Transmission Electron Microscopic (TEM) images of assembly **A** showing plate-like morphologies on silicon wafer for SEM and carbon grid for TEM. (e-f) SEM images of assembly **B** exhibiting twisted fibers on silicon wafer.

References

[1] I. Horcas, R. Fernández, J. M. Gómez-Rodríguez, J. Colchero, J. Gómez-Herrero, A. M. Baro, WSXM: A software for scanning probe microscopy and a tool for nanotechnology. *Rev. Sci. Instrum.* 2007, **78**, 013705.

[2] M. Yoshida, T. Hirao, T. Haino, Self-assembly of neutral platinum complexes possessing chiral hydrophilic TEG chains. *Org. Biomol. Chem.*, 2021, **19**, 5303-5311.

[3] T. Hirao, H. Tsukamoto, T. Ikeda, T. Haino, AIE-active micelles formed by self-assembly of an amphiphilic platinum complex possessing isoxazole moieties. *Chem. Commun.*, 2020, **56**, 1137-1140.

[4] (a) M. M. J. Smulders, A. P. H. J. Schenning, E. W. Meijer, *J. Am. Chem. Soc.*, 2008, **130**, 606-611. (b) M. M. J. Smulders, M. M. L. Nieuwenhuizen, T. F. A. de Greef, P. van der Schoot, A. P. H. J. Schenning, E. W. Meijer, *Chem. Eur. J.*, 2010, **16**, 362-367.